

RADC-TR-89-388  
Final Technical Report  
March 1990

AD-A220 780



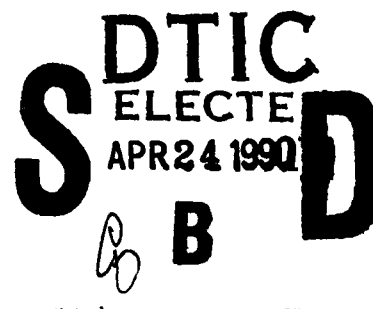
2

# REMOTE OPTICAL SENSING

Syracuse University

Dr. Philipp Kornreich

APPROVED FOR PUBLIC RELEASE; DISTRIBUTION UNLIMITED.



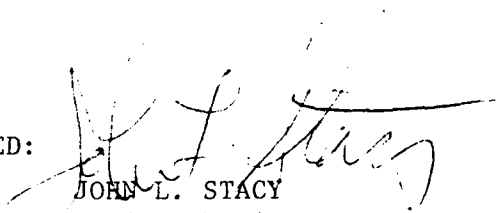
Rome Air Development Center  
Air Force Systems Command  
Griffiss Air Force Base, NY 13441-5700

90 04 19 137

This report has been reviewed by the RADC Public Affairs Division (PA) and is releasable to the National Technical Information Service (NTIS). At NTIS it will be releasable to the general public, including foreign nations.


RADC-TR-89-388 has been reviewed and is approved for publication.

APPROVED:



JOHN L. STACY  
Project Engineer

APPROVED:



DONALD W. HANSON  
Acting Director  
Photonics Laboratory

FOR THE COMMANDER:



BILLY G. OAKS  
Directorate of Plans & Programs

If your address has changed or if you wish to be removed from the RADC mailing list, or if the addressee is no longer employed by your organization, please notify RADC (OPA) Griffiss AFB NY 13441-5700. This will assist us in maintaining a current mailing list.

Do not return copies of this report unless contractual obligations or notices on a specific document require that it be returned.

UNCLASSIFIED  
SECURITY CLASSIFICATION OF THIS PAGE

| REPORT DOCUMENTATION PAGE   |       |   |  | Form Approved<br>OMB No. 0704-0188                  |                                  |
|---|-------|---|--|---|----------------------------------|
| 1a. REPORT SECURITY CLASSIFICATION<br>UNCLASSIFIED  |       |   | 1b. RESTRICTIVE MARKINGS<br>N/A  |   |                                  |
| 2a. SECURITY CLASSIFICATION AUTHORITY<br>N/A  |       |   | 3. DISTRIBUTION/AVAILABILITY OF REPORT<br>Approved for public release; distribution unlimited. |   |                                  |
| 2b. DECLASSIFICATION/DOWNGRADING SCHEDULE<br>N/A  |       |   |  |   |                                  |
| 4. PERFORMING ORGANIZATION REPORT NUMBER(S)<br>N/A  |       |   | 5. MONITORING ORGANIZATION REPORT NUMBER(S)<br>RADC-TR-89-388                                  |   |                                  |
| 6a. NAME OF PERFORMING ORGANIZATION<br>Syracuse University  |       | 6b. OFFICE SYMBOL<br>(if applicable)        | 7a. NAME OF MONITORING ORGANIZATION<br>Rome Air Development Center (OPA)                       |   |                                  |
| 6c. ADDRESS (City, State, and ZIP Code)<br>Department of Elec. and Computer Engineering<br>Syracuse NY 13244  |       |   | 7b. ADDRESS (City, State, and ZIP Code)<br>Griffiss AFB NY 13441-5700                          |   |                                  |
| 8a. NAME OF FUNDING/SPONSORING ORGANIZATION<br>Rome Air Development Center  |       | 8b. OFFICE SYMBOL<br>(if applicable)<br>OPA | 9. PROCUREMENT INSTRUMENT IDENTIFICATION NUMBER<br>F30602-88-D-0027, Task No. P80009           |   |                                  |
| 8c. ADDRESS (City, State, and ZIP Code)<br>Griffiss AFB NY 13441-5700   |       |   | 10. SOURCE OF FUNDING NUMBERS  |   |                                  |
|   |       |   | PROGRAM ELEMENT NO.<br>62702F  | PROJECT NO.<br>4600                                 | TASK NO.<br>P2                   |
|   |       |   |  |   | WORK UNIT ACCESSION NO.<br>P2    |
| 11. TITLE (Include Security Classification)<br>REMOTE OPTICAL SENSING   |       |   |  |   |                                  |
| 12. PERSONAL AUTHOR(S)<br>Dr. Philipp Kornreich   |       |   |  |   |                                  |
| 13a. TYPE OF REPORT<br>Final  |       | 13b. TIME COVERED<br>FROM Jun 88 TO Sep 89  |  | 14. DATE OF REPORT (Year, Month, Day)<br>March 1990 |                                  |
|   |       |   |  | 15. PAGE COUNT<br>44                                |                                  |
| 16. SUPPLEMENTARY NOTATION<br>N/A   |       |   |  |   |                                  |
| 17. COSATI CODES  |       |   | 18. SUBJECT TERMS (Continue on reverse if necessary and identify by block number)              |   |                                  |
| FIELD   | GROUP | SUB-GROUP                                   |  |   |                                  |
| 09  | 05    |   | Optical Image Transmission   |   |                                  |
| 20  | 06    | 01  | Graded Index Systems   |   |                                  |
| 19. ABSTRACT (Continue on reverse if necessary and identify by block number)<br>One of the major advantages of optical systems is their ability to process a great deal of information in parallel. The optical system discussed here transmits a complete image through a single optical fiber. This transmission system preserves the three-dimensional and color information of the image. The resolution is limited by the number of modes that can propagate in the fiber. The image is inserted and retrieved from the fiber by tapered input and output sections connected to the ends of the fiber. We built and tested a prototype image transmission system. We successfully transmitted a standard AF target through the system. We here present an analysis of how an image propagates through such a system. The model is derived from the electro-magnetic field equations. The image transmitted through the fiber does not necessarily have to be a picture of a real physical object. It could consist of various bits of information transmitted through the fiber in parallel. The transverse electric as well as the magnetic field modes propagate in the structure at different speeds. However, at periodic intervals all modes are in phase. At these points, |       |   |  |   |                                  |
| 20. DISTRIBUTION/AVAILABILITY OF ABSTRACT<br><input checked="" type="checkbox"/> UNCLASSIFIED/UNLIMITED <input type="checkbox"/> SAME AS RPT. <input type="checkbox"/> DTIC USERS   |       |   | 21. ABSTRACT SECURITY CLASSIFICATION<br>UNCLASSIFIED   |   |                                  |
| 22a. NAME OF RESPONSIBLE INDIVIDUAL<br>John L. Stacy  |       |   | 22b. TELEPHONE (Include Area Code)<br>(315) 330-2937   |   | 22c. OFFICE SYMBOL<br>RADC (OPA) |

UNCLASSIFIED

the image is in focus. The distance between these points is almost independent of the light wavelength. It only depends on the fractional change in the index of refraction ( $\Delta n/n_0$ ). Thus, this distance is almost independent of chromatic dispersion of the material. The distance the image can be transmitted through the fiber, at present, is limited by distortions and losses in the fiber.

|                    |  |
|--------------------|--|
| Accession For      |  |
| NTIS GRA&I         | <input checked="checked" type="checkbox"/> |
| DTIC TAB           | <input type="checkbox"/>                   |
| Unannounced        | <input type="checkbox"/>                   |
| Justification      |  |
| By                 |  |
| Distribution/      |  |
| Availability Codes |  |
| Dist               | Avail and/or<br>Special                    |
| A-1                |  |

UNCLASSIFIED

## 1 INTRODUCTION

One of the major advantages of optical systems is their ability to process a great deal of information in parallel. The optical system discussed here transmits a complete image, in parallel, through a single fiber. It is a passive system. **This transmission system preserves the three-dimensional and color information of the image.** The resolution of the image transmitted through the system is limited by the number of modes that can propagate in the fiber. The image is inserted and retrieved from the fiber by tapered input and output sections connected to the ends of the fiber, as shown in Fig. 1. We here present a theoretical analysis of how an image propagates through such a system. We analyze the propagation through both the tapered input and output sections as well as the light propagation through the fiber.

The large number of modes that can propagate through a large diameter graded index fiber and the propagation of optical signals with exceedingly low loss through modern fibers make this system possible.

The image is projected on the large face of a tapered graded index section. The core diameter of the large face of the tapered graded index section is, typically, 5 mm. The small end of the tapered section has the same core diameter and index of refraction profile as the graded index fiber to which it is attached. The tapered section is typically 20 cm's long. Such a tapered section has a linear magnification of 50. A typical graded index fiber in this application has a core diameter of about 100  $\mu\text{m}$ 's. The system is designed in such a way that the light intensity is about 60.6216 dB less at the edge of the graded index core than at the point where the maximum electric field occurs. As we shall see, the electro-magnetic field modes that carry the image information propagate with different velocities. However, periodically along the

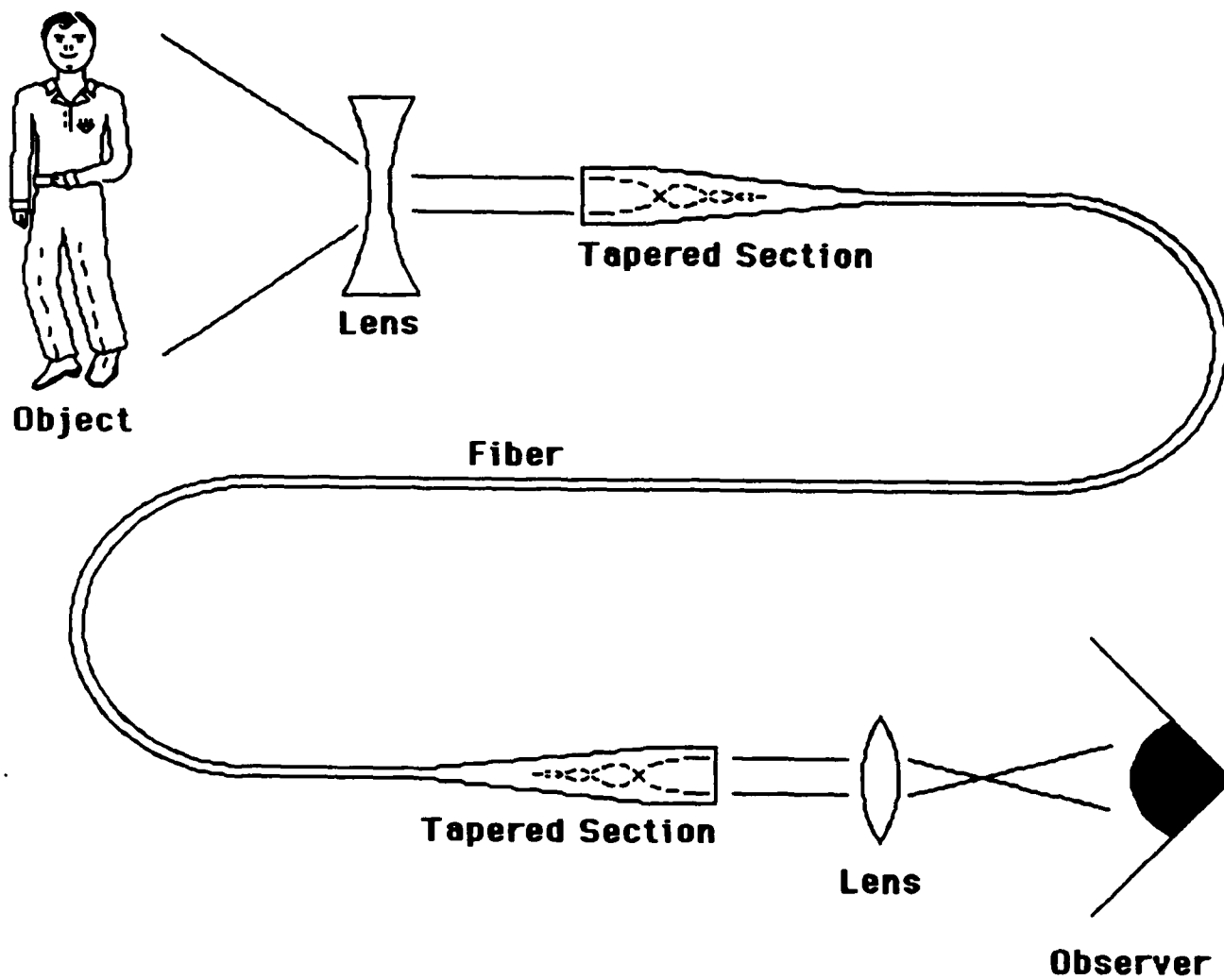


Fig. 1. Single fiber parallel image transmission system.

graded index structure the modes are in phase. At these points the image is in focus. Since the distance between points where the image is in focus depends only on the fractional change of the index of refraction ( $\Delta n/n_0$ ) along the radius and some geometric factor there should be little chromatic aberration in this system<sup>1</sup>. By placing the photo-detector at such an image point one should be able to detect modulated light without distortion.

A limitation of such a system is that it has a theoretical, numeric aperture of only 0.0127416 and therefore a very limited acceptance angle of about  $0.592^\circ$ . Thus, a concave lense has to be used to insert the image as shown in Fig. 1. The distance the image can be transmitted through the fiber and preserve the three-dimensional nature of the image is limited by distortions and losses in a fiber.

The system has advantages over systems where the image is divided into individual pixels and transmitted over a bundle of many fibers. In a fiber bundle image transmission system the resolution is limited by the number of fibers in the bundle<sup>2</sup>. The maintenance of the alignment of the fibers over the length of such a bundle system, is of course very critical. The fiber bundle system does not preserve the three-dimensional nature of the image. However, it does preserve the color information. The resolution in a single fiber system is mainly limited by the number of modes that can propagate in the fiber. It is also limited by the size of the aperture of the input and output sections.

H. Kita and T. Uchida<sup>3</sup> demonstrated that an image can be transmitted through curved graded index rods. They also discuss focusing of images by graded index rods and the transmission of an image through fiber bundles.

The light emanating from the image transmission system can be used

directly in an optical information processing system to extract information from the image. For example, the optical information processing system attached to the output of the image transmission system can be used to recognize certain patterns in the image.

The image transmitted through the fiber does not necessarily have to be a picture of a real physical object. It could consist of various bits of information that are transmitted through the fiber in parallel.

The most common methods for transmitting information through a fiber are; direct modulation of the light intensity by an electrical signal, pulse position modulation, and wavelength multiplexing. We here propose a spatial position multiplexing information transmission system.

It is possible to build a repeater for the single fiber image transmission system using a Micro-Channel Plate photomultiplier light amplifier. However, the use of such a light amplifier will cause the loss of the three-dimensional part of the image information.

It should, theoretically, be possible (in the future) to amplify the image using a Nd doped fiber light amplifier. Such light amplifiers exist. They are pumped by costreaming short wave length light. However, at present there are few lasers available that would conveniently produce the correct short wave length light. If this image light amplification is possible the image can be distributed over a number of fibers. One would then have a **true 3-D TV system** where the image is distributed through fibers.

The image arrives as an electro-magnetic field pattern at the large face of the tapered input section. The electro-magnetic field pattern can be thought of as being composed of the electric and magnetic field modes of the graded index system. These electric and magnetic field modes then propagate through the system. We shall, analyze the modes and their propagation properties in the below.

Gilbert H. Owyang in his book entitled "Foundations of Optical Wave



Guides"<sup>4</sup> gives a fairly extensive description of the modes and dispersion relation of a graded index structure. Ditrich Marcuse gives a less detailed description of the modes and dispersion relation in graded index structures in his book entitled "Light Transmission Optics"<sup>5</sup> However, the discussion of the modes and dispersion relations in these books are oriented towards optical communication by the use of a few modes and the descriptions are not quite sufficient for the analysis of image transmission. Greg Keiser in his book entitled "Optical Fiber Communications"<sup>6</sup>, Y. Suematsu and Ken-Ichi Iga in their book entitled "Introduction to Optical Fiber Communication"<sup>7</sup> and M. D. Freit and J. A. Fleck in their paper entitled "Light Propagation in Graded-Index Optical Fibers"<sup>8</sup> give a brief theory of electro-magnetic field modes propagating in graded index rods. N. Amitay and H. M. Presby<sup>9</sup> use a numerical method based on a model of successive lenses for a graded index sections and the two-dimensional Fourier transform of the electric field pattern to analyze the propagation of the fundamental mode in straight and tapered graded index sections. N. Amitay and H. M. Presby<sup>9</sup> also analyze the propagation of the fundamental mode in tapered and straight step index structures. These descriptions are somewhat simplified. They do not consider the exact nature of the wave equation for the electric field that has a direction perpendicular to the propagation direction. Nor do they consider the exact nature of the angular dependence of the modes in graded index systems. The spatial part of the wave equation as derived from Maxwell's equations contains more terms than are listed in these publications and, therefore, a more complete description of the modes of the electric and magnetic fields is required to describe the propagation of an image.

## 2 WAVE PROPAGATION

### 2a The Wave Equation

We will assume that the electric or magnetic fields have decayed to a negligible values at the core cladding interface. Therefore, we will neglect the effect of the core-cladding boundary on the modes of the electric and magnetic fields. The electric and magnetic field pattern of the light wave propagating in the graded index structure can be determined from the solution of the wave equation of the electric and magnetic fields. The wave equations can be derived from Maxwell's equations. Maxwell's equations have the following form in a medium with no electrical charge or current.

$$\nabla \times \mathbf{E} + \frac{\partial \mathbf{B}}{\partial t} = 0 \quad (2-1)$$

$$\nabla \times \mathbf{B} = [\mu_0 \epsilon_0 \epsilon(r, z)] \frac{\partial \mathbf{E}}{\partial t} \quad (2-2)$$

$$\nabla \cdot \mathbf{B} = 0 \quad (2-3)$$

$$\nabla \cdot \mathbf{D} = 0 \quad \text{or} \quad \nabla \cdot [\epsilon_0 \epsilon(r, z) \mathbf{E}] = 0 \quad (2-4)$$

where  $\mathbf{E}$  is the electric field vector,  $\mathbf{B}$  is the magnetic flux density vector  $\mu_0$  is the permeability of free space,  $\epsilon_0$  is the dielectric constant of free space, and  $\epsilon(r, z)$  is the spatially varying relative dielectric function of the material. We assume that the relative dielectric function varies both radially and along the optical axis of the graded index structures discussed here. The optical axis coincides with the z-axis of

the coordinate system used here. We shall assume that the relative dielectric function is a very gradually varying function of the coordinates. In this case equation 2-4 can be rewritten as follows:

$$\epsilon_0 \epsilon(r, z) \nabla \cdot \mathbf{E} \approx 0 \quad (2-5)$$

We shall, first, investigate modes in which the electric field is transverse to the direction of propagation of the wave, the TE modes. In order to derive the wave equation for these modes we take the curl of equation 2-1 and the time derivative of equation 2-2:

$$\nabla \times \nabla \times \mathbf{E} + \frac{\partial}{\partial t} \nabla \times \mathbf{B} = 0 \quad (2-6)$$

$$\frac{\partial}{\partial t} \nabla \times \mathbf{B} = [\mu_0 \epsilon_0 \epsilon(r, z)] \frac{\partial^2 \mathbf{E}}{\partial t^2} \quad (2-7)$$

By substituting  $\partial(\nabla \times \mathbf{B})/\partial t$  from equation 2-7 into equation 2-6 and making use of equation 2-5 and a vector identity for the double curl operator (equation 2-9) we obtain the wave equation for the electric field vector  $\mathbf{E}$  of the light wave:

$$\nabla^2 \mathbf{E} = [\mu_0 \epsilon_0 \epsilon(r, z)] \frac{\partial^2 \mathbf{E}}{\partial t^2} \quad (2-8)$$

where

$$\nabla^2 \mathbf{E} \equiv \nabla(\nabla \cdot \mathbf{E}) - \nabla \times \nabla \times \mathbf{E} \quad (2-9)$$

Let us assume that the wave propagates in the  $z$  direction and the electric field vector  $\mathbf{E}$  has components in the  $r$  and  $\theta$  directions only. That is, the electric field is perpendicular to the direction of propagation of the wave, see Fig. 2. These are the so called transverse electric field vector or TE modes. Once the electric field vector has been calculated the corresponding magnetic flux density vector  $\mathbf{B}$  for these modes can be determined from equation 2-1.

One can alternatively assume that the  $z$  direction propagating wave has a magnetic flux density vector  $\mathbf{B}$  with components in the  $r$  and  $\theta$  direction only. That is, the flux density vector is perpendicular to the direction of propagation of the wave. These are the so called transverse magnetic field or TM modes. Once the flux density vector has been calculated the corresponding electric field vector  $\mathbf{E}$  for these modes can be determined from equation 2-2. One will obtain a wave equation for the components of the magnetic flux density vector of the TM modes that is similar in form to the one for the electric field components of the TE modes. In a real light wave both type of modes are usually present. With these assumptions the equation 2-8 takes the following form in cylindrical coordinates:

$$\frac{1}{r} \frac{\partial}{\partial r} \left( r \frac{\partial E_r}{\partial r} \right) + \frac{1}{r^2} \frac{\partial^2 E_r}{\partial \theta^2} + \frac{\partial^2 E_r}{\partial z^2} - \frac{E_r}{r^2} - \frac{2}{r^2} \frac{\partial E_\theta}{\partial \theta} = [\mu_0 \epsilon_0 \epsilon(r, z)] \frac{\partial^2 E_r}{\partial t^2} \quad (2-10)$$

and

$$\frac{1}{r} \frac{\partial}{\partial r} \left( r \frac{\partial E_\theta}{\partial r} \right) + \frac{1}{r^2} \frac{\partial^2 E_\theta}{\partial \theta^2} + \frac{\partial^2 E_\theta}{\partial z^2} - \frac{E_\theta}{r^2} + \frac{2}{r^2} \frac{\partial E_r}{\partial \theta} = [\mu_0 \epsilon_0 \epsilon(r, z)] \frac{\partial^2 E_\theta}{\partial t^2} \quad (2-11)$$

where  $E_r$  and  $E_\theta$  are the radial and angular components of the electric

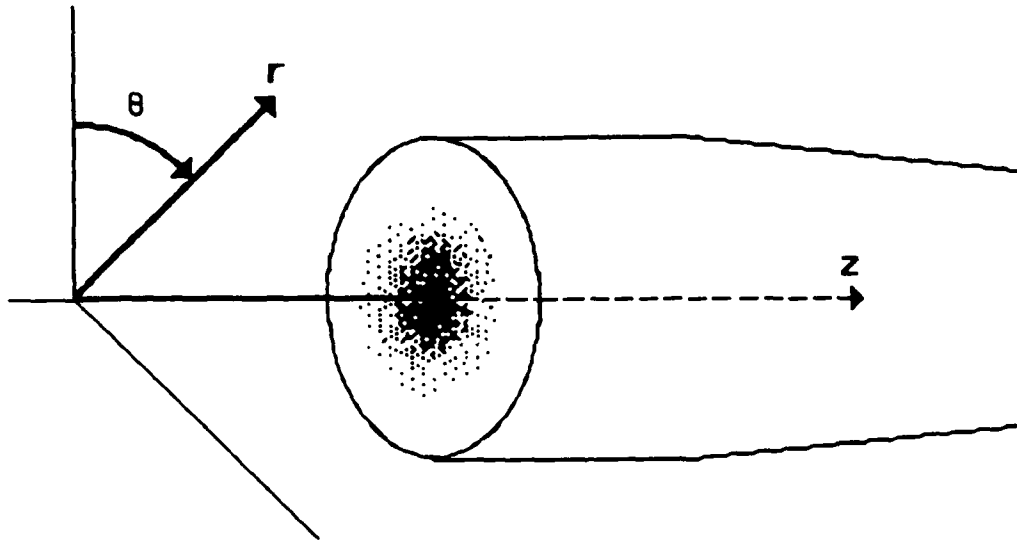


Fig. 2. The cylindrical coordinate system used here.

field vector respectively. The electric field components in equations 2-10 and 2-11 must also satisfy equation 2-5:

$$[\mu_0 \epsilon_0 \epsilon(r, z)] \left[ \frac{1}{r} \frac{\partial}{\partial r} (r E_r) + \frac{1}{r} \frac{\partial E_\theta}{\partial \theta} \right] = 0 \quad (2-12)$$

## 2b Solutions of the Wave Equation

We assume the following traveling wave solution for  $E_r$  and  $E_\theta$ :

$$E_p = \epsilon_p(r) e^{i[\omega t - m\theta - k(z)z]} \quad (2-13)$$

where the subscript  $p$  stands for either  $r$  or  $\theta$ , and  $\omega$  is the angular frequency of the light wave. Here  $m$  is an integer since the solution for the electric field at an angle of zero degrees and  $2m\pi$  radians must be identical. The wave vector  $k(z)$  is assumed to be a gradually varying

function of  $z$ . We assume the following form of the relative dielectric function for the cylindrically symmetric optical wave guide.

$$\epsilon(r,z) = \epsilon_c \left( 1 - \Delta \frac{r^2}{a^2(z)} \right) \quad (2-14)$$

where  $\Delta$  is the peak relative dielectric constant difference between the center and the point where  $r=a(z)$ , and  $a(z)$  is the radial taper function which is gradually varying with  $z$ . Let us use the following normalized coordinates:

$$\rho \equiv r \frac{\omega n_0}{c}, \quad \rho_0 \equiv a \frac{\omega n_0}{c}, \quad \text{and} \quad q \equiv \frac{k(z)c}{\omega n_0} \quad (2-15)$$

$$\text{where } c = \frac{1}{\sqrt{\mu_0 \epsilon_0}} \quad \text{and} \quad n_0 \equiv \sqrt{\epsilon_c}$$

By substituting equations 2-13, 2-14 and 2-15 into the wave equations, equations 2-10 and 2-11, we obtain:

$$\frac{1}{\rho} \frac{\partial}{\partial \rho} \left( \rho \frac{\partial \epsilon_r}{\partial \rho} \right) - \left( \frac{m^2+1}{\rho^2} - 1 + \Delta \frac{\rho^2}{\rho_0^2(z)} \right) \epsilon_r + \frac{2im}{\rho^2} \epsilon_\theta = q_{N,m}^2(z) \epsilon_r \quad (2-16)$$

and

$$\frac{1}{\rho} \frac{\partial}{\partial \rho} \left( \rho \frac{\partial \epsilon_\theta}{\partial \rho} \right) - \left( \frac{m^2+1}{\rho^2} - 1 + \Delta \frac{\rho^2}{\rho_0^2(z)} \right) \epsilon_\theta - \frac{2im}{\rho^2} \epsilon_r = q_{N,m}^2(z) \epsilon_\theta \quad (2-17)$$

where we assumed that the square of the normalized wave vector of the  $Nm$ 'th mode  $q_{N,m}^2(z)$  varies sufficiently gradually with  $z$  so that the derivatives of  $q_{N,m}^2(z)$  can be neglected. One can determine the radial dependence of the electric field components from equation 2-16 and 2-17. We assume the following solution for the components of the electric field:

$$\epsilon_p = \sum_N \epsilon_{pNm} \rho^\alpha \exp\left(-\frac{\rho^2}{2\sigma^2}\right) \sum_{n=0}^{n=N} b_{Nm n} \rho^{2n} \quad (2-18)$$

and

$$\begin{aligned} \frac{\partial \epsilon_p(\rho)}{\partial \rho} = \sum_N \epsilon_{pNm} \exp\left(-\frac{\rho^2}{2\sigma^2}\right) & \left[ -\frac{\rho^{\alpha+1}}{\sigma^2} + \alpha \rho^{\alpha-1} + \right. \\ & \left. b_{Nm1} \left( (2 + \alpha) \rho^{\alpha+1} - \frac{\rho^{\alpha+3}}{\sigma^2} \right) + \dots \right] \end{aligned} \quad (2-19)$$

where, as before, the subscript  $p$  stands for either  $r$  and  $\theta$ , and where  $\alpha$  will be calculated later. The solution  $\epsilon_p(\rho)$  of the differential equations as well as the derivatives of the solutions  $\partial \epsilon(\rho)/\partial \rho$  go to zero as  $\rho$  goes to infinity. At the center of the graded index structure, at  $\rho$  equal to zero, the derivatives of the solutions go to zero.

We multiply equations 2-16 by  $\rho^2$  and equation 2-17 by  $2im\rho^2$ . We, next, solve the equation resulting from equation 2-16 for  $2im\epsilon_\theta$ . We substitute the expression resulting from equation 2-16 for  $2im\epsilon_\theta$  into the expression derived from equation 2-17. We, lastly, divide the

resulting equation by  $\rho^4$  to obtain:

$$\left\{ \frac{1}{\rho} \frac{\partial}{\partial \rho} \left( \rho \frac{\partial}{\partial \rho} \right) - \left[ \frac{m^2 + 1}{\rho^2} - 1 + \Delta \frac{\rho^2}{\rho_0^2} + q_{Nm}^2(z) \right] \right\}^2 \mathcal{E}_r - \frac{4m^2}{\rho^4} \mathcal{E}_r = 0 \quad (2-20)$$

This requires that:

$$\frac{1}{\rho} \frac{\partial}{\partial \rho} \left( \rho \frac{\partial \mathcal{E}_r}{\partial \rho} \right) - \left[ \frac{m^2 + 1}{\rho^2} - 1 + \Delta \frac{\rho^2}{\rho_0^2(z)} \right] \mathcal{E}_r \pm \frac{2m}{\rho^2} \mathcal{E}_r = q_{Nm}^2(z) \mathcal{E}_r \quad (2-21)$$

A similar equation can be derived for the angular component  $\mathcal{E}_\theta$  of the electric field. The electric field components also have to satisfy equation 2-12. However, We shall postpone the discussion of this requirement until later.

The solution for the Nm'th mode of the radial component of the electric field can symbolically be written as  $\psi_{Nm}(\rho)$ . We substitute the solution for the Nm'th mode of the electric field for  $\mathcal{E}_r$  into equation 2-20 and multiplying the resulting equation by the solution of the Mm'th mode  $\psi_{Mm}(\rho)$ . We also substitute the solution for the Mm'th mode of the electric field for  $\mathcal{E}_r$  into equation 2-20 and multiplying the resulting equation by the solution of the Nm'th mode  $\psi_{Nm}(\rho)$ .

$$\psi_M \frac{1}{\rho} \frac{\partial}{\partial \rho} \left( \rho \frac{\partial \psi_N}{\partial \rho} \right) - \left[ \frac{(m \pm 1)^2}{\rho^2} - 1 + \Delta \frac{\rho^2}{\rho_0^2(z)} \right] \psi_M \psi_N = q_{Nm}^2(z) \psi_M \psi_N \quad (2-22)$$



$$\psi_N \frac{1}{\rho} \frac{\partial}{\partial \rho} \left( \rho \frac{\partial \psi_M}{\partial \rho} \right) - \left[ \frac{(m \pm 1)^2}{\rho^2} - 1 + \Delta \frac{\rho^2}{\rho_o^2(z)} \right] \psi_N \psi_M = q_{Mm}^2(z) \psi_N \psi_M \quad (2-23)$$

We, next, subtract equation 2-23 from equation 2-22 and integrate the result by parts.

$$\left[ \rho \psi_M \frac{\partial \psi_N}{\partial \rho} - \rho \psi_N \frac{\partial \psi_M}{\partial \rho} \right]_0^\infty = [q_{Nm}^2(z) - q_{Mm}^2(z)] \int_0^\infty \rho d\rho \psi_N \psi_M \quad (2-24)$$

Since the derivatives of the solution for the electric field are equal to zero at  $\rho$  equal to zero and both the derivatives and the solutions are equal to zero at  $\rho$  equal to infinity and since  $q_{Nm}^2(z)$  in general is not equal to  $q_{Mm}^2(z)$  the integral of the product of the solutions must be equal to zero for mode numbers  $N$  not equal to  $M$ . That is, the modes of the electric field are orthogonal. Indeed, we require a set of orthogonal modes in which the incident electric field pattern representing the image can be expanded. The above process is the Sturm-Liouville problem<sup>11</sup>.

By substituting equation 2-17 into equation 2-20, canceling  $\rho^\alpha$  and the Gaussian terms on both side of the equation we obtain:

$$\sum_{n=0}^{n=N} b_{nm} \left\{ [(2n + \alpha)^2 - (m \pm 1)^2] \rho^{2n-2} - \left[ \frac{4n + 2 + \alpha}{\sigma^2} - 1 \right] \rho^{2n} + \left( \frac{1}{\sigma^4} - \frac{\Delta}{\rho^2} \right) \rho^{2n+2} \right\} = q_{Nm}^2(z) \sum_{n=0}^{n=N} b_{nm} \rho^{2n} \quad (2-25)$$

We, next, rewrite equation 2-25 in expanded form:

$$\begin{aligned}
 & b_{N,m} \left\{ [(2N + \alpha)^2 - (m \pm 1)^2] \rho^{2N-2} - \left[ \frac{4N + 2 + \alpha}{\sigma^2} - 1 \right] \rho^{2N} + \right. \\
 & \left. \left( \frac{1}{\sigma^4} - \frac{\Delta}{\rho_o^2(z)} \right) \rho^{2N+2} \right\} + \\
 & b_{N-1,m} \left\{ [(2N - 2 + \alpha)^2 - (m \pm 1)^2] \rho^{2N-4} - \left[ \frac{4N - 2 + \alpha}{\sigma^2} - 1 \right] \rho^{2N-2} + \right. \\
 & \left. \left( \frac{1}{\sigma^4} - \frac{\Delta}{\rho_o^2(z)} \right) \rho^{2N} \right\} + \dots + \\
 & b_{n+1,m} \left\{ [(2n + 2 + \alpha)^2 - (m \pm 1)^2] \rho^{2n} - \left[ \frac{4n + 6 + \alpha}{\sigma^2} - 1 \right] \rho^{2n+2} + \right. \\
 & \left. \left( \frac{1}{\sigma^4} - \frac{\Delta}{\rho_o^2(z)} \right) \rho^{2n+4} \right\} + \\
 & b_{n,m} \left\{ [(2n + \alpha)^2 - (m \pm 1)^2] \rho^{2n-2} - \left[ \frac{4n + 2 + \alpha}{\sigma^2} - 1 \right] \rho^{2n} + \right. \\
 & \left. \left( \frac{1}{\sigma^4} - \frac{\Delta}{\rho_o^2(z)} \right) \rho^{2n+2} \right\} + \dots + \\
 & [\alpha^2 - (m \pm 1)^2] \rho^{-2} - \left[ \frac{2 + \alpha}{\sigma^2} - 1 \right] + \left( \frac{1}{\sigma^4} - \frac{\Delta}{\rho_o^2(z)} \right) \rho^2 = q_{N,m}^2(z) \sum_{n=0}^{N} b_{n,m} \rho^{2n}
 \end{aligned}
 \tag{2-26}$$

We collect terms of equal power of  $\rho$  where  $b_{om}$  is equal to one ( $b_{om} = 1$ ).

By setting the coefficient of  $\rho^{2N+2}$  equal to zero we obtain:

$$\frac{1}{\sigma^4} - \frac{\Delta}{\rho_o^2(z)} = 0 \quad \text{or} \quad \frac{1}{\sigma^2} = \frac{\sqrt{\Delta}}{\rho_o^2(z)} \quad (2-27)$$

Note that in general the variance  $\sigma^2$  is  $z$  dependent. For a conical graded index section with a gradually decreasing  $\rho_o$  or  $\alpha$  the variance  $\sigma^2$  also decreases. By setting the coefficient of  $\rho^{-2}$  equal to zero we obtain:

$$\alpha^2 - (m \pm 1)^2 = 0 \quad \text{or} \quad \alpha = \pm (m \pm 1) \quad (2-28)$$

By setting the coefficient of  $\rho^{2N}$  equal to zero we obtain the following form of the normalized wave vector of the  $Nm$ 'th mode:

$$q_{N,m}^2(z) = 1 - \frac{2\sqrt{\Delta}[2N + 1 \pm (m \pm 1)]}{\rho_o} \quad (2-29)$$

In order for the wave to propagate through the fiber the normalized wave vector  $q_{Nm}(z)$  must be real. The normalized wave vector  $q_{Nm}(z)$  will be real if the second term in equation 2-29 is smaller than one. This limits the sum  $[2N + 2 + m]$  of the number of radial and angular modes. This limits the resolution of the image that can be transmitted through the fiber. We used the plus sign for the angular mode number  $m$  and the "1" following it since, as we shall see, modes with negative  $m$  and "1" do not converge at  $\rho$  equal to zero and thus can not be used to describe the electric field in the fiber.

By setting the coefficient of  $\rho^{2N}$  equal to zero we obtain the following recursion relation for the polynomial coefficients  $b_{nm}$ :

$$b_{n+1,m} = - \frac{\sqrt{\Delta}[N-n]}{\rho_0(n+1)[(n+1) \pm (m \pm 1)]} b_{n,m} \quad (2-30)$$

## 2c Properties of the Radial Solution of the Wave Equation

From the above we conclude that the radial part of the wave equation has the following form:

$$\varepsilon_p(\xi) = \frac{\varepsilon_{pN,m}}{A_{N,m}} \exp\left(-\frac{\xi^2}{2}\right) \xi^{\pm m \pm 1} \sum_{n=0}^{n=N} b_{n,m} \xi^{2n} \quad (2-31)$$

where:

$$\xi \equiv \sqrt{\frac{\sqrt{\Delta}}{\rho_0}} \rho, \quad \text{or} \quad \xi = \sqrt{\frac{2\pi\sqrt{\Delta}}{\lambda_0 a}} r, \quad \text{or} \quad \xi = \frac{r}{\sigma} \quad (2-32)$$

and the subscript  $p$ , as before, stands for either  $r$  or  $\theta$ . Here  $A_{N,m}$  is a normalization constant which we shall calculate below. **The radial functions  $\varepsilon_p(\xi)$  of equation 2-31 are orthogonal for different radial mode numbers  $N$  and the same value of the angular mode number  $m$ .** With the help of the recursion relation of equation 2-30 and the fact that  $b_{0m}$  is equal to one we can construct the polynomial coefficients  $b_{nm}$ . The coefficients of the polynomials have the following form:

$$b_{n,m} = (-1)^n \frac{N!(m+1)!}{(N-n)!n!(n+m+1)!} \quad \text{for } m+1 > 0 \quad (2-33)$$

The first few associated Laguerre<sup>4</sup> polynomials are listed below:

$$H_0^{+m} = \xi^{m+1}$$

$$H_1^{+m} = \xi^{m+1} \left[ 1 - \frac{1}{2+m} \xi^2 \right]$$

$$H_2^{+m} = \xi^{m+1} \left[ 1 - \frac{2}{2+m} \xi^2 + \frac{1}{6+5m+m^2} \xi^4 \right]$$

$$H_0^{-m} = \xi^{1-m}$$

$$H_1^{-m} = \xi^{1-m} \left[ 1 - \frac{1}{2-m} \xi^2 \right]$$

$$H_2^{-m} = \xi^{1-m} \left[ 1 - \frac{2}{2-m} \xi^2 + \frac{1}{6-5m+m^2} \xi^4 \right]$$

$$K_0^{+m} = \xi^{m-1}$$

$$K_1^{+m} = \xi^{m-1} \left[ 1 - \frac{1}{m} \xi^2 \right]$$

$$K_2^{+m} = \xi^{m-1} \left[ 1 - \frac{2}{m} \xi^2 + \frac{1}{m(m+1)} \xi^4 \right]$$

$$K_0^{-m} = \xi^{-m-1}$$

$$K_1^{-m} = \xi^{-m-1} \left[ 1 + \frac{1}{m} \xi^2 \right]$$

$$K_2^{-m} = \xi^{-m-1} \left[ 1 + \frac{2}{m} \xi^2 + \frac{1}{m(m-1)} \xi^4 \right]$$

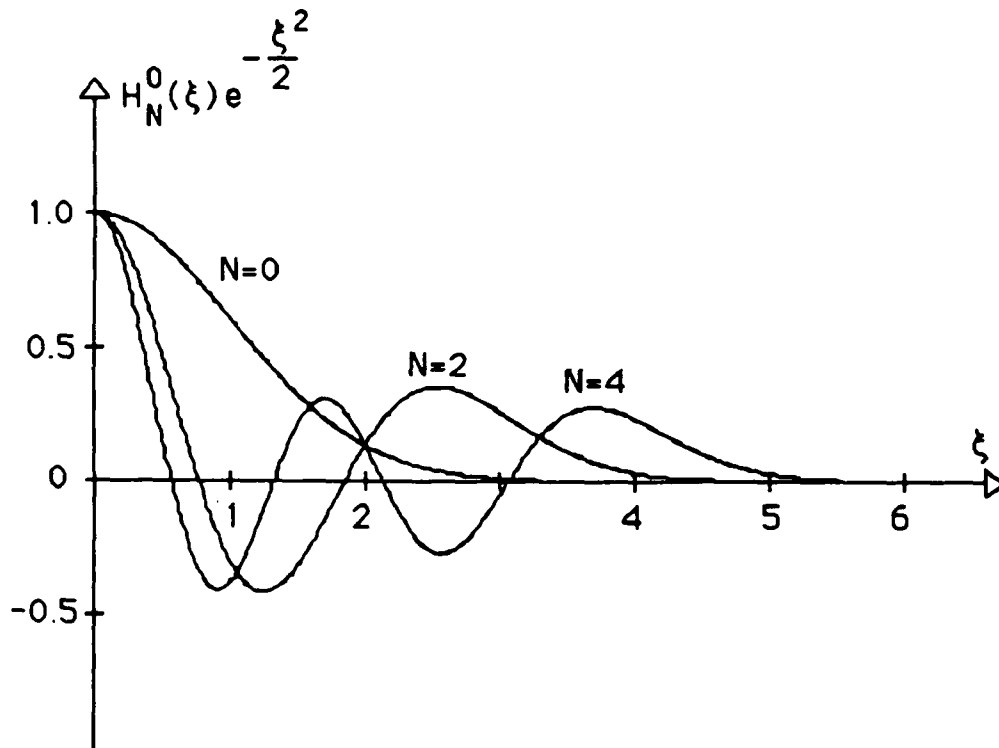


Fig. 3. Plot of the three functions  $H_0^0(\xi)$ ,  $H_2^0(\xi)$ , and  $H_4^0(\xi)$  times a Gaussian. The angular mode number  $m$  is equal to one and  $m+1=0$ .

We here assumed that  $\rho_0$  does not vary along the optical axis. This is the case for a cylindrical graded index section. We assume that  $m$  is a positive integer. With this assumption note that  $H_N^m$  has a singularity

at  $\xi$  equal to zero for  $m$  greater than one. Similarly,  $K_N^{+m}$  has a singularity at  $\xi$  equal to zero for  $m$  less than one, and  $K_N^{-m}$  has a singularity at  $\xi$  equal to zero for all values of  $m$ . As stated before, the functions  $H$  and  $K$  multiplied by a Gaussian are orthogonal for the same value of  $m$  and different values of  $N$ .

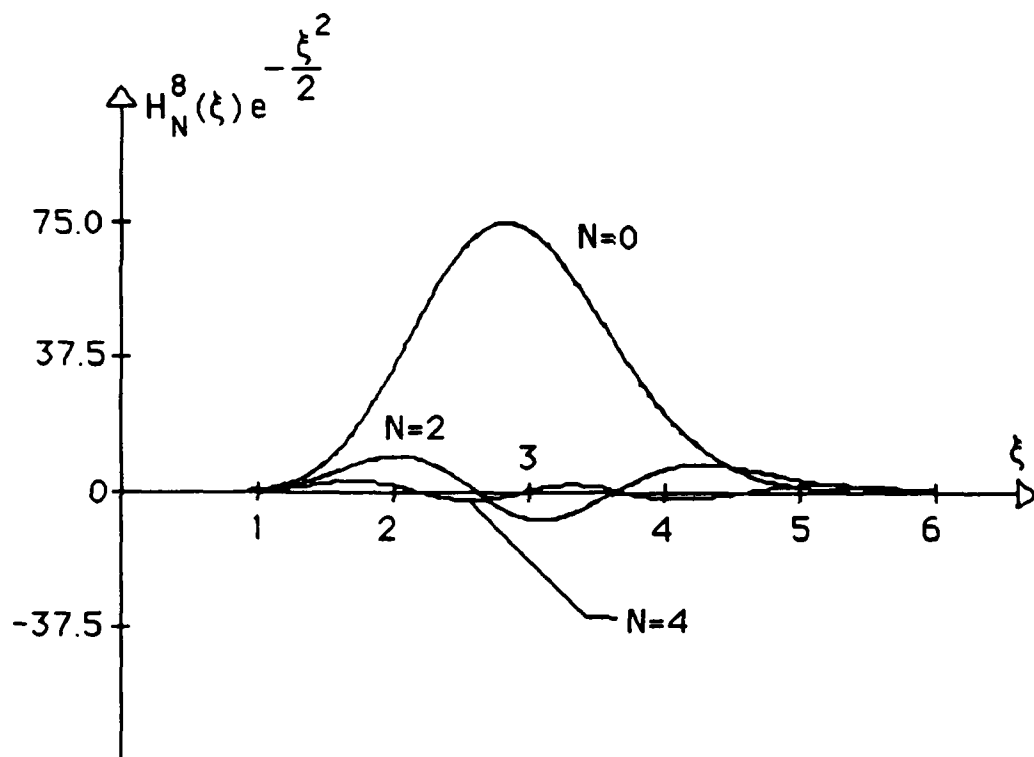


Fig. 4. Plot of the three functions  $H_0^8(\xi)$ ,  $H_2^8(\xi)$ , and  $H_4^8(\xi)$  times a Gaussian. The angular mode number  $m$  is equal to 7 and  $m+1=8$ .

Only functions that are not singular at  $\xi$  equal to zero and have derivatives that are equal to zero at  $\xi$  equal to zero describe modes of the electric field in the graded index structures. The same thing holds for the magnetic flux density of the TM modes. Some typical modal

solutions are plotted in figures 3 and 4. The fundamental mode consisting of a Gaussian only is shown in Fig. 3. In Fig. 4 we show the radial dependence of modes with a larger angular mode number. Modes with large angular mode numbers  $m$  are centered at a radial distance  $\xi = \sqrt{(m+1)}$ . The radial moding causes these modes to have oscillations centered at  $\xi = \sqrt{(m+1)}$ , see Fig. 4. The  $N=0$  modes with angular mode number  $m$  has a width in  $\xi$  that is approximately equal to  $\sqrt{2}$ .

We, next, calculate the normalization constants for the radial functions:

$$A_{N,m}^2 = \frac{1}{2} \sum_{k=0}^N \sum_{n=0}^N (-1)^{k+n} \frac{(N!)^2 [(m+1)!]^2}{[(N-n)!]^2 k! n! (k+m+1)! (n+m+1)!} \times \int_0^\infty e^{-x} x^{k+n+m+1} dx \quad (2-34)$$

where:

$$x \equiv \xi^2 \quad \text{and} \quad \frac{1}{2} dx = \xi d\xi \quad (3-35)$$

By integrating equation 2-34 we obtain for the normalization coefficients for the radial functions:

$$A_{N,m}^2 = \frac{(m+1)!}{2} \sum_{k=0}^N \sum_{n=0}^N (-1)^{k+n} \frac{N!}{k!(N-k)!} \frac{N!}{n!(N-n)!} \frac{(m+1)!(k+n+m+1)!}{(k+m+1)!(n+m+1)!} \quad (2-36)$$

By substituting equation 2-15 into 2-29 we obtain the following dispersion relation:



$$\frac{2\pi}{\lambda_{N,m}} = \frac{2\pi}{\lambda_0} \sqrt{1 - \frac{\sqrt{\Delta}\lambda_0[2N + 1 \pm (m \pm 1)]}{\pi a}} \quad (2-37)$$

where:

$$\frac{2\pi}{\lambda_0} \equiv \frac{\omega n_0}{c} \quad (2-38)$$

and where  $\lambda_{N,m}$  is the wave length of the N,m'th mode. Two adjacent modes that were in phase at one point along the fiber will again be in phase at a distance  $z_M(N,m)$  from that point. The phase shift between the two adjacent modes, say the Nm'th and (N+1),m'th mode, will differ by exactly  $2\pi(1+M)$  radians after they have propagated a distance  $z_M(N,m)$ . Since we are interested in **transmitting the image over a large distance** the distance  $z_M(N,m)$  will be of the order of, say, 100 m's and M will be a large integer. This can be expressed mathematically by using equation 2-37 as follows:

$$\begin{aligned} \frac{2\pi}{\lambda_0} \sqrt{1 - \frac{\sqrt{\Delta}\lambda_0[2N + 1 \pm (m \pm 1)]}{\pi a}} z_M(N,m) = \\ 2\pi(1 + M) + \frac{2\pi}{\lambda_0} \sqrt{1 - \frac{\sqrt{\Delta}\lambda_0[2N + 3 \pm (m \pm 1)]}{\pi a}} z_M(N,m) \end{aligned} \quad (2-39)$$

We note that each mode propagates with a different velocity. However, after both the Nm'th and (N+1),m'th modes have traveled a distance  $z_M(N,m)$  they will be in phase again. We note that  $2\pi a/\sqrt{\Delta}$  is much larger than  $\lambda_0$ . Therefore, for sufficiently small mode numbers the

square roots in equation 2-39 can be expanded to first order to yield:

$$z_M = \frac{\pi(1 + M)a}{\sqrt{\Delta}} \quad (2-40)$$

We note that in this approximation at a large distance  $z_M$  along the fiber the two adjacent Modes  $N,m$  and  $(N+1),m$  will be in phase. We also note that this large distance is independent of mode numbers  $N$  and  $m$ . Therefore, **in a transparent rod with a parabolically graded square of the index of refraction, a static image projected on the face of the rod will, also, be in focus at a large distance  $z_M$  of some hundreds of meters from the input face.** We note that the distance  $z_M$  is independent of the light wavelength. Also, the change in index of refraction  $\sqrt{\Delta}/a$ , on which  $z_M$  depends, is much less dependent upon the wavelength of the light propagating through the rod than is  $n_0^2$ . The shortest distance  $z_0$  at which a static image projected at the face of the rod will be in focus is at  $M=0$ :

$$z_0 = \frac{a\pi}{\sqrt{\Delta}} \quad (2-41)$$

We note that in this approximation the distance  $z_0$  that two adjacent modes have to propagate in order for them be in phase again is independent of the mode numbers  $N$  and  $m$ . Thus, at a distance  $z_0$  from the point where all the modes were in phase they will, approximately, be in phase again. Therefore, **in a transparent rod with a parabolically graded square of the index of refraction a static image projected on the**

face of the rod will be in focus approximately at periodic intervals with period  $z_0$ , see Fig. 5.

Newport Corporation<sup>11</sup> lists the characteristics of some graded index quarter pitch lenses (rods) in their GRIN-Rod Lens Starter Kit F-GRK1 instruction Manual. The quantity  $\sqrt{A}$  listed in this literature corresponds to the quantity  $\sqrt{\Delta/a}$  in this paper. The quarter pitch length,  $(1/4)P$ , in the Newport literature corresponds to the quantity  $z_0/2$  in our paper. In table 1 we compare the measured value from the Newport literature with the quantity  $z_0$  calculated from the quantity  $\sqrt{A}$  and equation 2-35. Observe the good agreement between measured,  $(1/4)$  Pitch, and calculated,  $z_0/2$ , values.

TABLE 1

| $\sqrt{A}$       | $(1/4)Pitch$ | $(a/\sqrt{\Delta})$ | $(z_0/2) = (1/4)Pitch$ |
|------------------|--------------|---------------------|------------------------|
| mm <sup>-1</sup> | in mm's      | in mm's             | in mm's                |
| Meas'd.          | Meas'd.      | Calc'd.             | Calc'd.                |
| 0.0964           | 16.3         | 10.273              | 16.295                 |
| 0.489            | 3.35         | 2.049               | 3.212                  |
| 0.247            | 6.5          | 4.049               | 6.360                  |
| 0.202            | 7.8          | 4.950               | 7.776                  |
| 0.601            | 2.6          | 1.664               | 2.614                  |
| 0.332            | 4.7          | 3.012               | 4.731                  |
| 0.298            | 5.25         | 3.356               | 5.271                  |
| 0.423            | 3.7          | 2.364               | 3.714                  |

Table 1. Comparison of experimentally measured and theoretically calculated quarter pitch length ( $z_0/2$ ) in graded index rods.

The variance  $\sigma^2(z)$  for the non-normalized coordinates as derived from equations 2-15 and 2-27, has the following form:

$$\sigma^2(z) = \frac{n(z)\lambda_0}{2\pi\sqrt{\Delta}} \quad (2-42)$$

The Gaussian beamwaist  $w_p(z)$  (of the fundamental mode) quoted by N. Amitay and H. M. Presby<sup>9</sup> in equation 3 of their publication is equal to two times the standard deviation  $\sigma(z)$ . The Gaussian beamwaist  $w_p(z)$  is also discussed in equation 7.3-21 of reference 5. We assume that, in general, both  $n(z)$  and  $\sigma^2(z)$  are gradually varying functions of  $z$ .

By subtracting equation 2-21 from equation 2-16 we obtain:

$$i\mathcal{E}_\theta = \pm \mathcal{E}_r \quad (2-43)$$

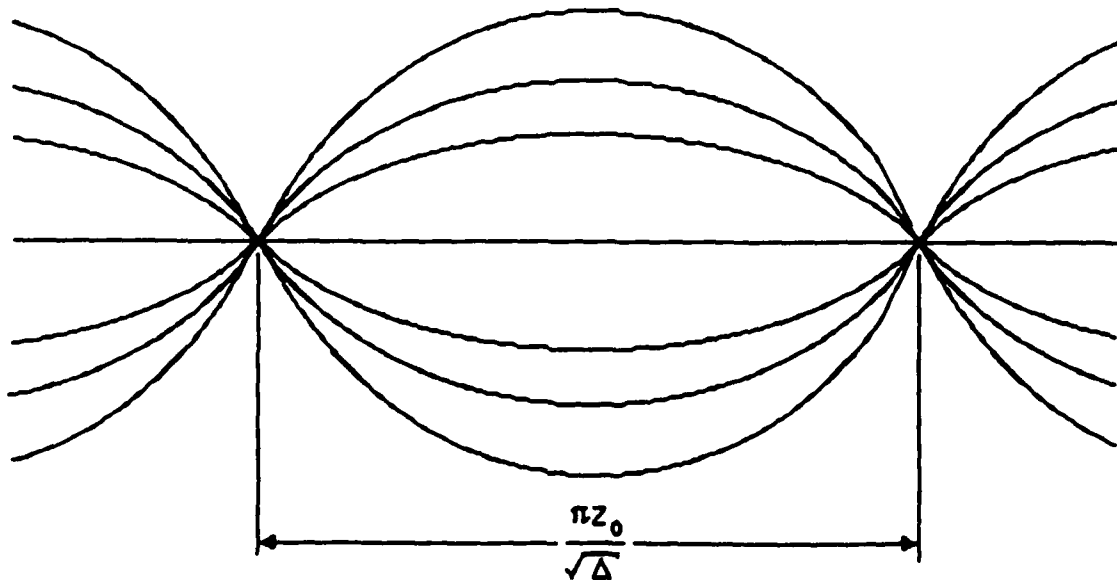


Fig. 5. Light ray path in a parabolically graded index rod.

This implies that the radial and angular electric field components are  $90^\circ$  out of phase. That is, the electric field vector rotates in a plane perpendicular to the optical axis of the graded index rod.

## 2d Number of Propagating Modes In an Image

The resolution of the image is determined by the number of modes available to transport the image. Since the fiber is the component with the smallest diameter it will restrict the number of modes that propagate through the system. The solutions to the wave equation that we have used here assume that the electric or magnetic fields have decayed to a negligible values at the core cladding interface. Therefore, the core-cladding boundary will have only a negligible effect on the modes. As we have seen only modes with  $m+1>0$  can describe electric or magnetic fields in the fiber. The maximum number of modes  $[2N + m + 2]_{\max}$  that can propagate in the fiber and come periodically to focus must satisfy the approximation used for the derivation of equations 2-40 and 2-41.

$$[2N + m + 2]_{\max} \approx \frac{\pi a}{4\sqrt{\Delta}\lambda_0} \quad (2-44)$$

where we made use of equations 2-15 and 2-38. The mode with the largest angular mode  $m_{\max}$  will have the largest radial extension of all the modes used. Therefore, we substitute equation 2-42 for  $a/\sqrt{\Delta}$  into equation 2-44 for the largest angular mode number  $m_{\max}$  that still satisfies the periodic focusing approximation.

$$m_{\max} + 2 \approx \frac{\pi^2 \sigma^2}{2\lambda_0^2} \quad (2-45)$$

The electric field at a radius  $R_0$ , at the core cladding interface, of the largest angular mode has the following form as derived from equation 2-31:

$$\epsilon_p(R_0) = \exp\left(-\frac{R_0^2}{2\sigma^2}\right) \left(\frac{R_0}{\sigma}\right)^{m+1} \quad (2-46)$$

Here, as before, the subscript  $p$  stands for either  $r$  or  $\theta$ . The peak value of the electric field of this mode occurs at:

$$r_{\max} = \sigma\sqrt{m+1} \quad (2-47)$$

and

$$\epsilon_{p,\max} = \left[\frac{m+1}{e}\right]^{\frac{m+1}{2}} \quad (2-48)$$

where  $e$  is the base of the natural logarithm. We require that the electric field at the core cladding interface of the fiber be about 60 dB less than at its maximum value:

$$-60 = 20 \log \frac{\epsilon_p(R_0)}{\epsilon_{p,\max}} \quad (2-49)$$

By combining equations 2-45, 2-46, 2-47, 2-48, and 2-49 we obtain:

$$-60 = -20 \left[ \frac{\pi^2 R_0^2}{4\lambda_0^2(m+2)} - \frac{m+1}{2} \right] \log(e) + 10 \log(m+1) \log \left( \frac{\pi^2 R_0^2}{2\lambda_0^2} \right) - 10(m+1) \log[(m+1)(m+2)] \quad (2-50)$$

The largest value  $m_{\max}$  of the angular mode number consistent with the assumption necessary to have periodic focusing of the image in the graded index section can be calculated from equation 2-50.

The numeric aperture NA of a graded index lense is defined as<sup>11</sup>:

$$NA \equiv \frac{n_0 R_0 \sqrt{\Delta}}{a} \quad (2-51)$$

The specifications and properties of a typical graded index image transmission system operating with light having a wavelength of 520 nm's in vacuum are listed in table 2. In column 4 of table 2 we list the properties of the Newport/NSG graded index rod-lens with the largest quarter pitch length from table 1 for comparison. A 100  $\mu\text{m}$  diameter fiber drawn from this lense would only permit a maximum number of  $m_{\max} = 12$  modes to be transmitted.

The linear magnification of the image in the fiber by the tapered graded index section is equal to 50. This requires that the ratio of the standard deviation in the large diameter graded index section to the

TABLE 2

| Parameter                     | Fiber                          | Large Dia.<br>Section          | Newport/NSG<br>Grin Rod*       |
|-------------------------------|--------------------------------|--------------------------------|--------------------------------|
| $n_o$                         | 1.556                          | 1.556                          | 1.596                          |
| $R_o$                         | 50 $\mu\text{m}'\text{s}$      | 2.5 mm's                       | 1 mm                           |
| $a/\sqrt{\Delta}$             | 122.120 $\mu\text{m}'\text{s}$ | 305.299 mm's                   | 10.273 mm's                    |
| $\sigma$                      | 2.54859 $\mu\text{m}'\text{s}$ | 127.429 $\mu\text{m}'\text{s}$ | 23.0804 $\mu\text{m}'\text{s}$ |
| $z_o$                         | 0.383650 mm's                  | 959.126 mm's                   | 32.2736 mm's                   |
| $m_{\text{max}}$<br>for $N=0$ | 285                            | 285**                          | 1653**                         |
| $m_{\text{max}}$<br>for $N=m$ | 95                             | 95**                           | 551**                          |
| NA                            | 0.637080                       | 0.0127416                      | 0.155359                       |
| PR***                         | -60.6216 dB                    | -60.6216 dB                    | -60.6434 dB                    |
| $r_{\text{max}}$              | 43.1006 $\mu\text{m}'\text{s}$ | 2.15503 mm's                   | 0.938666 mm's                  |

\*See Table 1.

\*\*Calculated from the requirement that the electric field of the largest angular mode to be about 60 dB less at the core-cladding interface than at its maximum value which occurs at  $r_{\text{max}}$ .

\*\*\*Here  $PR = 20\log[\mathcal{E}(R_o)/\mathcal{E}_{p\text{max}}]$

Table 2. Typical specifications of a Single Graded Index Fiber Image transmission System.

standard deviation in the fiber to be equal to 50. The "magnification



$\alpha''$  quoted in equation 2 by N. Amitay and H. M. Presby<sup>9</sup> as well as the ratio of the quantities  $\alpha/\sqrt{\Delta}$  are equal to the square of the linear magnification or to 2500. Here  $r_{\max}$  is the radial distance from the center of the graded index section to where the peak of the  $N=0$ ,  $m=m_{\max}$  mode occurs, see equation 2-47.

## 2e Dynamic Properties Of Images.

We have above discussed the propagation properties of a static image through the graded index system. We here consider the propagation properties of a time varying image.

The group velocity  $V$  is given by:

$$V = \frac{d\omega}{dk} \quad (2-52)$$

The group velocity for each mode can readily be calculated from equation 2-15 and 2-29. We obtain the following expression for the group velocity:

$$V = \frac{c}{n_0} \frac{1}{\sqrt{\frac{x_{N,m}^2}{1 - x_{N,m}} + 1}} \quad (2-53)$$

where:

$$x_{N,m} \equiv \frac{\sqrt{\Delta} \lambda_0 [2N + 1 \pm (m \pm 1)]}{\pi a} \quad (2-54)$$

One observes that the group velocity at constant wavelength depends on

the sum of the angular and radial mode numbers  $m$  and  $N$  respectively. In Fig. 6 we plot the percentage change of the group velocity for a constant light wavelength of 520 nm's in vacuum for a fiber as a function of the sum of the radial and angular mode numbers. We chose the same parameters for the fiber as in section 2d.

We are interested in the difference  $\Delta t$  in the propagation times of the fundamental mode, the mode with  $N=0$ ,  $m+1=0$ , and the highest angular mode, the mode with  $N=0$ ,  $m=m_{\max}$  in a fiber of length  $L$ :

$$\Delta t = \frac{L}{V(N=0, m=m_{\max})} - \frac{L}{V(N=0, m=0)} \quad (2-55)$$

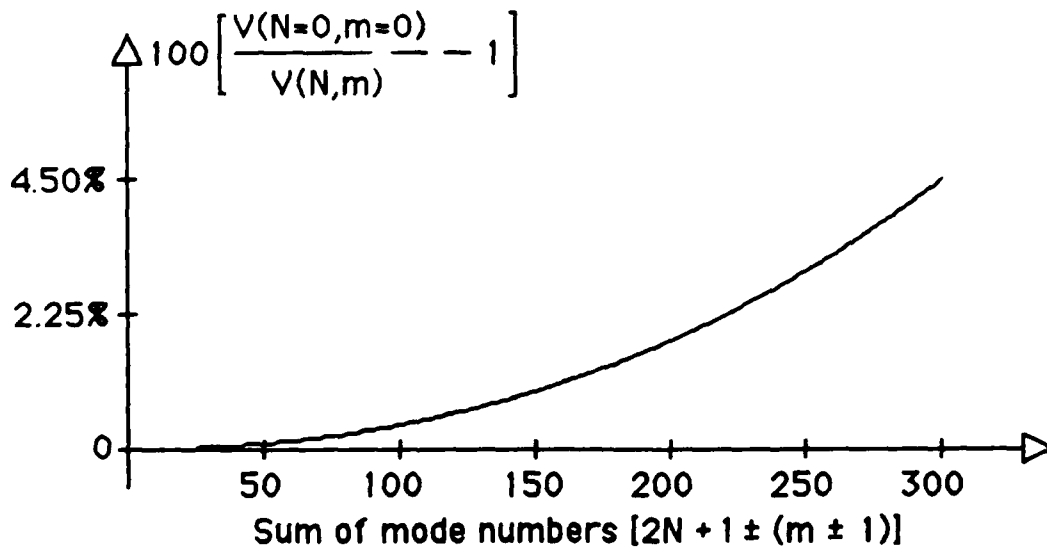


Fig. 6. Plot of the ratio of the percentage change of the group velocity as a function of the sum of the mode numbers in a fiber with a 100  $\mu\text{m}$  core diameter. Here  $\lambda_0 = 334.1902$  nm's.,  $V(N=0, m=0) = 1.926684 \times 10^8$  m/sec., and  $n_0 = 1.556$ .

For a 100 m long fiber with the specifications given in table 2,

operating with light with a wavelength of 520 nm's in vacuum  $\Delta t = 21.1925$  nsec. The image can be blinked on and off at a maximum frequency, approximately, equal to the reciprocal of  $\Delta t$  or 47.1866 Mhz.

## 2f Tapered Graded Index Section

D. Marcuse<sup>13</sup> calculated the effect of the taper in a graded index section upon the modes propagating through such a structure. We, however here simply assume that the taper is gradual enough so that these effects can be neglected. We assume the following form for the quantity  $a(z)/\sqrt{\Delta(z)}$ .

$$\frac{a(z)}{\sqrt{\Delta(z)}} = \frac{a_0}{\sqrt{\Delta_0}} \left\{ 1 + \frac{\beta - 1}{2} \left[ 1 + \tanh\left(\frac{z_{CT} - z}{z_D}\right) \right] \right\} \quad (2-56)$$

Where  $\Delta(z)$  is the peak relative dielectric constant difference between the center and the point where  $r=a(z)$ ,  $a(z)$  is the radial taper function which is gradually varying with  $z$ , and  $a_0/\sqrt{\Delta_0}$  is the value of  $a/\sqrt{\Delta}$  in the fiber. Here  $\beta$  is equal to the "magnification  $\alpha$ " quoted in equation 2 by N. Amitay and H. M. Presby<sup>9</sup>,  $z$  is the distance along the optical axis of the fiber and tapered section measured from the end of the large diameter section,  $z_{CT}$  is the distance from the end of the large diameter section to the center of the taper, and  $z_D$  is the "distance constant" of the taper function. The large diameter section ends and the taper starts at approximately  $z = z_{CT} - (3z_D)$ . The fiber "pig tail" starts at approximately  $z = z_{CT} + (3z_D)$ . We calculate the points along the optical axis where an image that is in focus at the face of the large diameter sections is, again, in focus. We assume here that  $z_{CT} = 150$  mm's,  $z_D = 43$

mm's, and  $\beta=2500$ . The results of this calculation using equations 2-40 and 2-56 are listed in table 3.

**TABLE 3**

| M   | $z_M$ mm's |
|-----|------------|
| 1   | 181.349    |
| 2   | 196.7214   |
| 3   | 205.2936   |
| 4   | 211.2712   |
| 5   | 2158.687   |
| 6   | 219.6078   |
| 7   | 222.7608   |
| 8   | 225.4881   |
| 9   | 227.8921   |
| 10  | 230.0421   |
| 110 | 280.90525  |
| 111 | 281.11589  |

Table 3. The distance from the input face of the large diameter section of a conical graded input section to points where the image would be in focus again if it is in focus at the input face.

We observe from table 3 that the distance between consecutive points where the image is in focus decreases drastically as the quantity  $\alpha/\sqrt{\Delta}$  decreases and as the taper approaches the dimensions of the fiber. At a distance of 281.11589 mm's from the face of the large diameter section the quantity  $\alpha/\sqrt{\Delta}$  has reached a value of 806.144  $\mu$ m's. It is interesting to note that one would predict a half pitch value  $z_0$  of

2.53258 mm's for the above value of  $\alpha/\sqrt{\Delta}$ . However, the difference between  $z_{111}$  and  $z_{110}$  is only 0.21064 mm's. A similar result can be obtained by a ray tracing technique that uses the matrices of reference 9. The ray tracing data is not presented in this paper. Perhaps, this is related to the light guide taper effect discussed in the August 1989 issue of Scientific American<sup>14</sup>. Recall from table 2 that in the fiber  $\alpha/\sqrt{\Delta}=122.120 \mu\text{m's}$ .

#### 4 CONCLUSION

We built and tested a prototype graded index image transmission model. The model consisted of a 0.5 mm diameter prototype fiber with ends that tapered to 5 mm diameter input and output sections. The structure was about 400 mm long. We successfully transmitted a standard Air Force Target through the system. There seem to be little loss in resolution.

#### 5 CONCLUSION

We have developed a theoretical model that explains how an image can be transmitted in parallel through a system consisting of a graded index fiber with graded index conical sections attached at its ends. The model is derived from the electro-magnetic field equations. It analyzes how the various electric field modes propagate through the system. The image arrives as an electric field pattern at the large face of the tapered input section. The electric field pattern can be thought of as being composed of the modes of the graded index system. These electric field modes then propagate through the system.

The image is inserted into a 5 mm diameter cylindrical graded index

section that tapers to a 100  $\mu\text{m}$  diameter graded index fiber. This taper provides a 50:1 linear demagnification. The numeric aperture of the large diameter section is equal to 0.0127416. The resolution of the system is limited by the small diameter fiber to only 285 radial and angular modes. The electric field of the 285'th radial mode is 60.622 dB less at the core cladding interface than at the point,  $r = 43.1006 \mu\text{m's}$ , where the peak of the largest angular mode occurs. The Gaussian associated with the electric and magnetic field modes in the fiber has a standard deviation  $\sigma = 2.54859 \mu\text{m's}$ . The propagation delay of the different modes limits the maximum rate of change of the image to approximately, 47.1866 MHz in a 100 m long fiber.

## REFERENCES:

1. "Contemporary Optics, Graded Index Optic" Notes by Duncan T. Moore, Data on p. 132, (1989), The Institute for Optics, College of Engineering and Applied Science, University of Rochester, Rochester, N. Y. 14627.
2. "Optical Fibers in Medicine" by Abraham Katzir, Scientific American, Vol. 260, No. 5, May 1989, pp 120-125.
3. "Light Focusing Glass Fiber and Rods" by H. Kita (Nipon Sheet Glass Co., Ltd., Osaka, Japan) and T. Uchida (Nipon Electric Co., Ltd., Kawasaki, Japan) Japan Annual Review in Electronics, Computers, and Telecommunication OPTICAL DEVICES AND FIBERS pp. 117-123.
4. "Foundations of Optical Wave Guides" by Gilbert H. Owyang,

5. "Light Transmission Optics" by Ditrich Marcuse, Second Edition, Von Nostrand Reinhold Company, New York, Toronto, INSB-0-442-20309-0 (1982)
6. "Optical Fiber Communications" by Greg Keiser, McGrow Hill Book Co. N. Y., St. Louis, San Francisco.
7. "Introduction to Optical Fiber Communications" by Yasuharu Suematsu, John Wiley and Sons Inc. N. Y. (1982).
8. "Light Propagation in Graded Index -Index Optical Fibers" by M. D. Freit and J. A. Fleck, Applied Optics, Vol. 17, pp 399-3998 Dec. 1978.
9. "Optical Fiber Up-Taper Modeling and performance Analysis" by N. Amitay and H. M. Presby, Journal of Lightwave Technology, Vol. 7, pp 131-137, January 1989.
10. "Current Status of Graded-Index Rod Lenses" by Ichiro Kitano (Research Laboratory, Nipon Sheet Glass Co. Ltd., Itami 664, Japan) Japan Annual Review in Electronics, Computers, and Telecommunication OPTICAL DEVICES AND FIBERS, Y Suematsu, Editor pp. 151-166.
11. "The Mathematics of Physics and Chemistry" by Henry Morgenau and George Moseley Murphy, D. Van Nostrand Company Inc. Princeton, N. J., Section 8.7.
12. Graded Index Rod Lenses, GRIN-Rod Lens Starter Kit F-GRK1 Instruction Manual, Newport Corporation Fiber Optics (Nipon

Sheet Glass), 18235 Mt. Bakly Circle, Founyain Valley, CA, 92708, p 5, Table 1, (1988).

13. "Mode Conversion in Optical Fibers with Monotonically Increasing Core Radius" by Ditrich Marcuse, Journal of Lightwave Technology, Vol. LT-5 pp. 125-133, 1, January 1987.
14. TECHNOLOGY "Bring Me Sunshine" by T. M. B. Scientific American, Vol. 261, pp. 20-21 August 1989.

### FIGURE CAPTIONS:

Fig. 1. Single fiber parallel image transmission system.

Fig. 2. The cylindrical coordinate system used here.

Fig. 3. Plot of the three functions  $H_0^0(\xi)$ ,  $H_2^0(\xi)$ , and  $H_4^0(\xi)$  times a Gaussian. The angular mode number  $m$  is equal to one and  $m+1=0$ .

Fig. 4. Plot of the three functions  $H_0^8(\xi)$ ,  $H_2^8(\xi)$ , and  $H_4^8(\xi)$  times a Gaussian. The angular mode number  $m$  is equal to 7 and  $m+1=8$ .

Fig. 5. Light ray path in a parabolically graded index rod.

Fig. 6. Plot of the ratio of the percentage change of the group velocity as a function of the sum of the mode numbers in a fiber with a 100  $\mu\text{m}$  core diameter. Here  $\lambda_0 = 334.1902 \text{ nm's.}$ ,  $V(N=0,m=0)=1.926684 \times 10^8 \text{ m/sec.}$ , and  $n_0 = 1.556$ .

### TABLE CAPTIONS:



Table 1. Comparison of experimentally measured and theoretically calculated quarter pitch length ( $z_0/2$ ) in graded index rods.

Table 2. Typical specifications of a Single Graded Index Fiber Image transmission System.

Table 3. The distance from the input face of the large diameter section of a conical graded input section to points where the image would be in focus again if it is in focus at the input face.